

Anodization of Aluminum: New applications for a common technology

Anodization is a common technology to passivate aluminum surfaces and the appearance of randomly distributed pores in the surface is well known and used to stain the surface in a second step. In 1995 Masuda et al. reported a two step anodization which leads to a regular distribution of the pores due to a self-organization process [1]. This induced a rising interest in these pores as they offer structures in the nanometer scale which can be used in applications for magnetic storage [2], solar cells [3], carbon nanotubes [4], catalysts [5] and metal nanowires [6]. Their use as substrates for artificial lipid membranes [7] will be outlined within this report.

Introduction

In ambient conditions aluminum surfaces are naturally covered by a thin alumina (Al_2O_3) layer. The thickness of this layer is about several tens of nanometers. With the anodization technique the layer thickness can be increased to some microns. In that way the surfaces are more resistant against salt water, slightly acidic solutions or scratches. Anodization is commonly used for corrosion protection of aluminum and there are international standards (ISO 7599, DIN 17611, BS 3987, etc.) regulating quality and thickness of anodized surfaces.

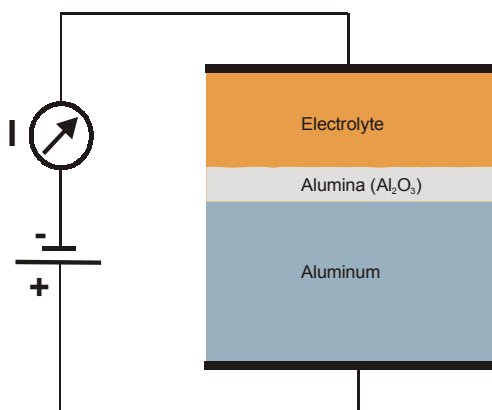


Figure 1: Scheme of the setup for the anodization of Aluminum. The aluminum part is contacted to the anode of an electrical circuit in an acidic electrolyte while a counterelectrode in the electrolyte is contacted to the cathode.

Normally, anodization is done by applying an electrical current to a part of aluminum in an acidic electrolyte as depicted in Figure 1. Anodization leads to an alumina layer with a porous surface. As this is objectionable for corrosion protection, the surface is being welling after the anodization, e.g. by immersing the part in boiling water.

Creating ordered nanoporous surfaces

In the last decades intensive studies led to new insights to the principles underlying the anodization processes and helped refining the methods to prepare porous surfaces. The appearance of pores during anodization depends on the oxidation rate of aluminum and the field-enhanced oxide dissolution rate at the oxide/electrolyte interface [8]. Both depend on the applied electrical field strength and the chosen electrolyte, which have to be adjusted properly to create homogeneous pores.

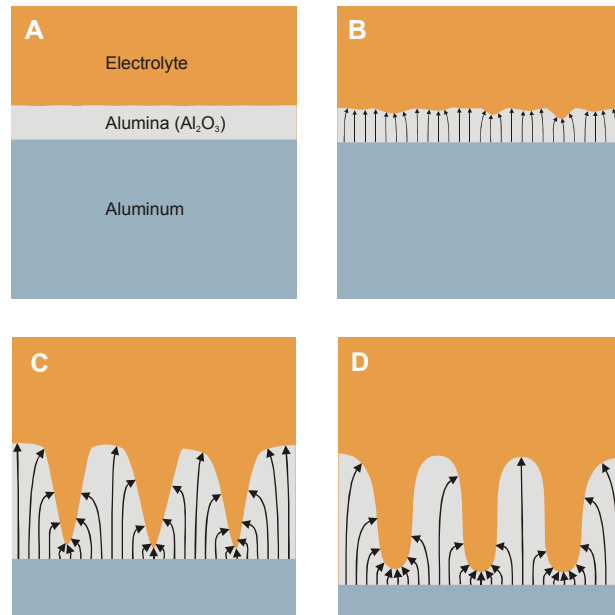


Figure 2: Stages in the development of porous alumina during anodization.

As depicted in Figure 2, the application of an electric field first leads to the development of a compact barrier layer of alumina (A). Small topographic differences within this

layer cause inhomogenities in the applied electrical field as indicated by arrows (B). This increases the dissolution rate of the oxide locally. Small pores are deepened further, while the electrical field and the dissolution rate in the alumina between two pores decreases (C). Deep pores continuously “grow” during the ongoing anodization (D) with a speed of 1 – 2 $\mu\text{m/h}$.

The interpore distances can be adjusted in the range of 50 – 420 nm with the applied potential [9]. Anodization at low potetials (30 – 60 V) in 0.3 M oxalic acid at 2 °C leads to pore distances of 50 – 150 nm. Potentials of 100 - 160 V can be applied using 10 wt% phosphoric acid as electrolyte at 3 °C and lead to interpore distances of 300 – 420 nm. As a rule of thumb, the pore diameter can be estimated to be 30% of the interpore distance [10]. It can be increased if the surface is chemically etched after the anodization.

At the beginning of the anodization process, the pores are randomly distributed on the surface. During their growth into the bulk material they arrange in a hexagonal pattern due to a process of self organisation. This can be utilized to create surfaces with ordered pores: The primarily created oxide layer is removed (e.g. in an aqueous solution of 6 wt% phosphoric acid and 1.8 wt% Cr(VI)oxide) and a second anodization process is carried out using the pre-structured aluminum surface as template [11].

Imaging Nanoporous Alumina Surfaces

To characterize the porous surfaces Scanning Electron Microscopy (SEM) or Atomic Force Microscopy (AFM) are used. Figure 3 shows ordered nanoporous alumina surfaces prepared by the described twofold anodization with a potential of 40 V in oxalic acid and subsequent chemical etching in oxalic acid for 3 h at 30 °C. Even small irregularities in the surface structure of the pore rims are visible in the AFM image.

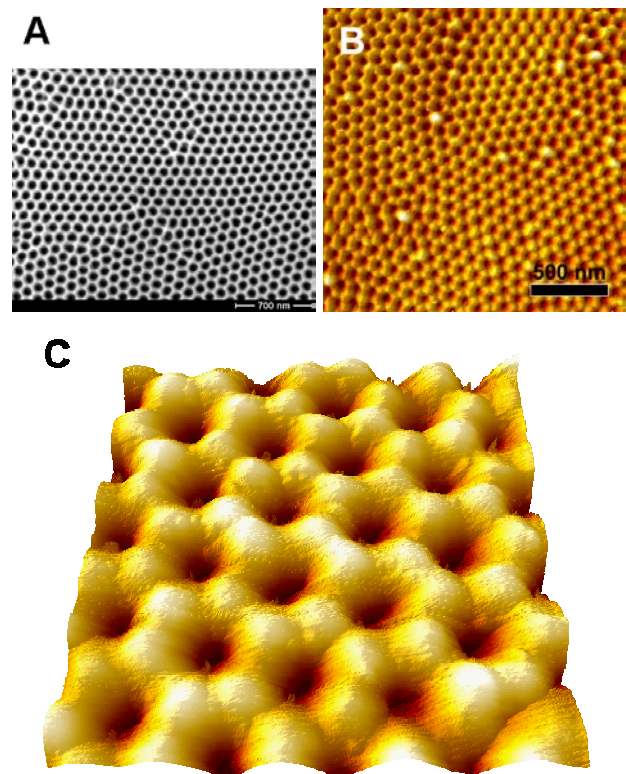


Figure 3: Comparison of a SEM image (A) and AFM images (B) and (C) of nanoporous alumina. There are neighbouring areas with different orientations of perfectly ordered hexagonal lattices. Point defects in the lattices appear as bright humps in the AFM image (B). Details in the structure of the pore rims are visible in the AFM image (C) of an $0.5 \times 0.5 \mu\text{m}^2$ array. The color scales correspond to height differences of $\approx 75 \text{ nm}$ for (B) and $\approx 50 \text{ nm}$ for (C).

Application of Nanoporous Alumina Surfaces as Substrates for Pore-suspending Lipid Membranes

As an example for the application of ordered nanopores their use as substrates for pore-suspending lipid membranes [7] will be outlined.

In this application the porous alumina surface was negatively functionalized to allow fusion of positively charged lipid vesicles onto the porous substrate. A scetch of the vesicle fusion on the functionalized surface is shown in Figure 4.

The lipid of choice was *N,N*-dimethyl-*N,N*-dioctadecylammonium bromide (DODAB) as it binds electrostatically on 3-mercaptopropionic acid at pH 8.6.

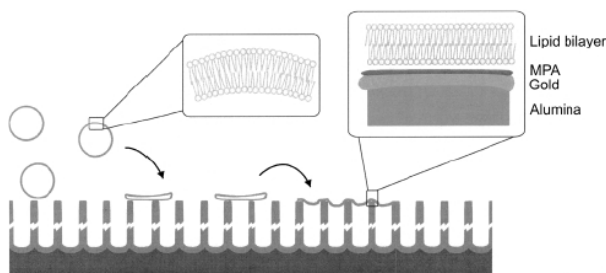


Figure 4: Schematic drawing (taken from [7]) of the preparation of pore-suspending lipid bilayers obtained from fusion of positively charged large unilamellar vesicles on a 3-mercaptopropionic acid monolayer. The vesicle and pore sizes are drawn to scale; the lipid bilayer with a thickness of only 5 ± 6 nm is drawn thicker.

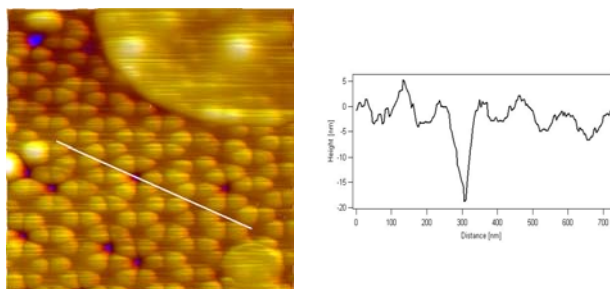


Figure 5: AFM image (array: $1 \times 1 \mu\text{m}^2$, height scale: 40 nm) of membrane covered pores scanned with a tip force of 0.5 nN in buffer solution (10 mM Tris, pH 8.6). Pores which appear deeper than -15 nm are coloured in blue. The height profile of the indicated scan line shows the different apparent depth of six pores in a row.

The existence of pore-suspending membranes could be verified as the membranes showed elastic deformation during subsequent AFM-scans with different loading forces. Figure 5 shows an example image scanned with a small loading force of 0.5 nN. The area with the smooth surface in the top right corner corresponds to a multilayer stack of lipid. The honeycomb structure of the alumina is clearly visible throughout the rest of the image. Z-values deeper than -15 nm appear blue in the image. These few

areas may not be covered by lipid. The main fraction of the pores appear in different shades of brown and the apparent depth of these pores differs with the applied loading force of the AFM tip. This leads to the conclusion that most but not all pores are spanned by a lipid membrane, which can be reversibly deformed by the AFM tip. More details can be found in [7].

Literature

- [1] Masuda H., Fukuda K.: Ordered metal Nanohole Arrays Made by a Two-Step Replication of Honeycomb Structures of anodic Alumina. *Science* 268, 1466 – 1468, **1995**
- [2] Nielsch K., Wehrspohn R.B., Barthel J., Kirschner J., Gösele U., Fischer S.F., Kronmüller H., *Applied Physics Letters* 79 (9), 1360 - 1362, **2001**
- [3] Karmhag R., Tesfamichael T., Wackelgard E., Niklasson G.A., Nygren M.: Oxidation Kinetics of Nickel Particles: Comparison between free Particles and Particles in an Oxide Matrix. *Solar Energy* 68 (4), 329 - 333, **2000**
- [4] Che G., Lakshmi B.B., Fisher E.R., Martin C.R.: Carbon Nanotubule Membranes and possible Applications to Electrochemical Energy Storage and Production. *Nature* 393, 346 - 347, **1998**
- [5] Che G., Lakshmi B.B., Martin C.R., Fisher E.R., Ruoff R.S.: Chemical Vapor Deposition (CVD)-Based Synthesis of Carbon Nanotubes and Nanofibers Using a Template Method. *Chemistry of Materials* 10 (1), 260 - 267, **1998**
- [6] Zhang Z.B., Gekhtmann D., Dresselhaus M.S., Ying J.Y.: Processing and Characterization of Single-Crystalline Ultrafine Bismuth Nanowires. *Chemistry of Materials* 11 (7), 1659 - 1665, **1999**
- [7] Hennesthal C., Drexler J., Steinem C.: Membrane-Suspended nanocompartments Based on Ordered Pores in Alumina. *ChemPhysChem* 10, 885 – 889, **2002**
- [8] Jessensky O., Müller F., Gösele U.: Self-organized formation of hexagonal pore arrays in anodic alumina. *Applied Physics Letters* 72 (10), 1173 – 1175, **1998**
- [9] Li A.P., Müller F., Birner A., Nielsch K., Gösele U.: Hexagonal pore arrays with 50 – 420 nm interpore distance formed by self-organization in anodic alumina. *Journal of Applied Physics* 84 (11), 6023 – 6026, **1998**
- [10] Nielsch K., Choi J., Schwirn K., Wehrspohn R.B., Gösele U.: Self-ordering Regimes of Porous Alumina. The 10% porosity Rule. *Nano Letters* 2 (7), 677 – 680, **2002**
- [11] Li A.P., Müller F., Birner A., Nielsch K., Gösele U.: Fabrication and microstructuring of hexagonally ordered two-dimensional nanopore arrays in anodic alumina. *Advanced Materials* 11, 483 - 487, **1999**